

Variationally stable treatment of two- and three-photon detachment of H^- including electron-correlation effects

Chih-Ray Liu*

Department of Physics and Astronomy, The University of Nebraska-Lincoln, Lincoln, Nebraska 68588-0111

Bo Gao and Anthony F. Starace†

Joint Institute for Laboratory Astrophysics, University of Colorado and National Institute of Standards and Technology, Boulder, Colorado 80309-0440

(Received 27 April 1992)

A variationally stable, adiabatic hyperspherical treatment of two- and three-photon detachment of H^- is presented. Results are compared with analytic predictions of a zero-range potential model of H^- . Detailed comparisons are made also with other theoretical results which include the effects of electron correlations. We predict analytically (and demonstrate numerically) an extreme sensitivity of the theoretical predictions to any errors in the value of the electron affinity employed. In an Appendix we show that the low-intensity limit of the Keldysh treatment [Sov. Phys. JETP **20**, 1307 (1965)] of detachment of an electron bound in a zero-range potential agrees with the results of a perturbative treatment.

PACS number(s): 32.80.Wr

I. INTRODUCTION

The hydrogen negative ion, which is a fundamental three-body system, has long served as a testing ground for new theoretical methods, including treatments of multiphoton detachment processes [1–7]. The recent experimental observation of multiphoton detachment of the H^- ion [8, 9] has kindled renewed theoretical interest [10–16]. However, as noted by Geltman [16(b)], the various theoretical predictions for the two- and three-photon detachment cross sections of H^- are quite disparate. While most theoretical works have described the H^- system as a one-electron system in which the active electron moves in a short-range potential, several of the theoretical calculations treat explicitly some of the two-electron correlations relevant to multiphoton detachment [3, 4, 7, 10, 13, 14]. Nevertheless, even among the results of only these more detailed theoretical treatments, disparities remain.

In this paper we present variationally stable predictions of the generalized cross sections [17] for two- and three-photon detachment of H^- . Electron correlations for these processes are treated within a semiempirical, adiabatic hyperspherical representation. Our variational procedure for calculating high-order multiphoton processes perturbatively [18, 19] has been applied extensively to H [18]. Recently, its implementation for two-electron systems described in the adiabatic hyperspherical representation [20–23] has been outlined and an application was made to the dynamic polarizability of He [19].

Fink and Zoller [4] have used the adiabatic hyperspherical representation to calculate the generalized cross section for two-photon detachment of H^- by circularly polarized light. Our calculations differ from theirs, firstly, in that we have used a variationally stable procedure [18, 19] to calculate the transition matrix elements. Secondly,

we have semiempirically adjusted the $1S^e$ hyperspherical potential curve so that the electron affinity of the initial state agrees exactly with the nonrelativistic electron affinity predicted by Pekeris [24].

Semiempirically adjusting the electron affinity to the correct value turns out to be extremely important for obtaining accurate generalized cross sections for multiphoton detachment processes. Using a one-electron, short-range potential model, for which one can obtain analytic predictions for the generalized multiphoton detachment cross sections [16(b)], one can estimate the importance of having the correct electron affinity. Thus, we show that if the electron affinity I is incorrect by an amount ΔI , then the N -photon detachment cross section may have a fractional error of as much as $(4N - 1)\Delta I / (I + \frac{1}{2}k^2)$, where $\frac{1}{2}k^2$ is the detached electron's kinetic energy. Thus, at a kinetic energy $\frac{1}{2}k^2$ for which the fraction $(\Delta\omega/\omega) \equiv \Delta I / (I + \frac{1}{2}k^2)$ is equal to 0.05, the five-photon detachment cross section may be in error by as much as 100%. For the two- and three-photon cross sections presented in this paper, our semiempirical adjustment of the $1S^e$ adiabatic hyperspherical ground-state potential reduces the peak value of the calculated cross sections by 25% and 40% respectively from the predictions obtained using the adiabatic hyperspherical value for the electron affinity.

We compare our generalized cross sections for two- and three-photon detachment of H^- with those of others which include electron-correlation effects. In place of comparing individually with the results of the many other theoretical calculations which employ a one-electron, short-range potential model of H^- , we compare our semiempirical, adiabatic hyperspherical results with results of our own zero-range potential model, whose analytic cross-section formulas we present. Geltman [16(b)] has shown that it is very important in the case of two-

photon detachment with linearly polarized light to take into account the $1S^e$ phase shift for the detached electron. Using the free-electron Green's function with outgoing-wave boundary conditions, we obtain the two-photon transition amplitude analytically in terms of the $1S^e$ phase shift. We show that above the one-photon threshold this transition amplitude is complex *except* when the $1S^e$ phase shift is zero. Our analytically-determined, phase-shifted, zero-range potential-model results for two-photon detachment by linearly polarized light agree well with the numerically determined results of Geltman. They are compared with our semiempirical adiabatic hyperspherical results.

Lastly, we have examined the question of how the lowest-order perturbation theory results presented here relate to results of calculations that take into account the exact interaction of the detached electron with the laser field. For the velocity gauge, Reiss [2] has shown that in the low-intensity limit the more general theoretical results reduce as expected to the results obtained by lowest-order perturbation theory. In this paper, however, we employ the length gauge, for which the exact final-state wave function for an electron moving in a laser field has been given by Keldysh [25]. As far as we are aware, the low-intensity limit of multiphoton photodetachment cross sections using the Keldysh final-state wave function has never been examined. In fact, Keldysh presented, in addition to his general result, a low-frequency approximation to his general result. This latter approximate formula has been found to disagree, in the low-intensity limit, with results of lowest-order perturbation theory [26]. For this reason, we prove that Keldysh's general result [25] reduces in the low-intensity limit to results of lowest-order perturbation theory, as one would expect.

In Sec. II we review briefly our variationally stable procedure for calculating the generalized cross sections for two- and three-photon detachment of H^- within an adiabatic hyperspherical representation. In Sec. III we present analytic expressions for the generalized cross sections for two- and three-photon detachment of H^- within a zero-range potential model. From these results we show the sensitivity of the theoretical N -photon detachment cross section to any errors in the electron affinity of the negative ion. In Sec. IV we present our analytic results for the two-photon detachment amplitude assuming there is a nonzero, final-state s -wave phase shift. In Sec. V we present our two- and three-photon generalized detachment cross section results for H^- and compare with results of others. In Sec. VI we discuss our conclusions regarding the role of electron correlations on multiphoton detachment of H^- . Finally, in the Appendix we present our results on the low-intensity limit of Keldysh-treatments for multiphoton detachment processes.

II. VARIATIONALLY STABLE TREATMENT IN THE ADIABATIC HYPERSPHERICAL REPRESENTATION

In this section we review briefly the hyperspherical coordinate representation for the H^- ion. We also review briefly our variationally stable procedure for perturbative calculations of multiphoton transition amplitudes. Interested readers are referred to Refs. [20–23] and [18, 19] respectively for more detailed descriptions of these two topics.

A. Adiabatic hyperspherical coordinate representation

In ordinary coordinate space, the H^- system is described nonrelativistically by the Hamiltonian

$$H = -\frac{1}{2}\nabla_1^2 - \frac{1}{2}\nabla_2^2 - \frac{1}{r_1} - \frac{1}{r_2} + \frac{1}{r_{12}}. \quad (1)$$

The hyperspherical coordinates $(R, \alpha, \hat{r}_1, \hat{r}_2)$ are defined by

$$R = (r_1^2 + r_2^2)^{1/2}, \quad \alpha = \tan^{-1}(r_2/r_1). \quad (2)$$

In this set of coordinates, the Hamiltonian becomes [20–23]

$$H = -\frac{1}{2} \left[\frac{\partial^2}{\partial R^2} + \frac{5}{R} \frac{\partial}{\partial R} - \frac{\Lambda^2}{R^2} + \frac{C}{R} \right], \quad (3)$$

where

$$\Lambda^2 = -\frac{1}{\sin^2 \alpha \cos^2 \alpha} \frac{d}{d\alpha} \sin^2 \alpha \cos^2 \alpha \frac{d}{d\alpha} + \frac{\hat{L}_1^2}{\cos^2 \alpha} + \frac{\hat{L}_2^2}{\sin^2 \alpha}, \quad (4)$$

$$C = \frac{2Z}{\sin \alpha} + \frac{2Z}{\cos \alpha} - \frac{2}{[1 - \sin(2\alpha) \cos \theta_{12}]^{1/2}}. \quad (5)$$

The adiabatic channel functions $\phi_\mu(R; \alpha, \hat{r}_1, \hat{r}_2)$ are defined as the eigenfunctions of the angular equation [20–23].

$$(-\Lambda^2 + RC)(\phi_\mu / \sin \alpha \cos \alpha)$$

$$= [U_\mu(R) + 4](\phi_\mu / \sin \alpha \cos \alpha), \quad (6)$$

in which R is treated as a parameter. The eigenvalue $U_\mu(R)$ forms a radial potential. The wave function can generally be written as the following expansion in the channel functions:

$$\psi = (R^{5/2} \sin \alpha \cos \alpha)^{-1} \sum_{\mu} F_{\mu}(R) \phi_{\mu}(R; \alpha, \hat{r}_1, \hat{r}_2), \quad (7)$$

where $F_{\mu}(R)$ satisfies

$$\left[\frac{d^2}{dR^2} + \frac{U_{\mu} + 1/4}{R^2} + \left(\phi_{\mu}, \frac{\partial^2}{\partial R^2} \phi_{\mu} \right) + 2E \right] F_{\mu}(R) + \sum_{\mu' (\neq \mu)} \left[\left(\phi_{\mu}, \frac{\partial^2}{\partial R^2} \phi_{\mu'} \right) + 2 \left(\phi_{\mu}, \frac{\partial}{\partial R} \phi_{\mu'} \right) \frac{d}{dR} \right] F_{\mu'}(R) = 0. \quad (8)$$

Clearly, each $F_\mu(R)$ is governed largely by the potentials $U_\mu(R)$, whereas the coupling between different channels is governed by the radial derivative matrix elements inside the sum over μ' .

In the adiabatic (or separable) approximation [20], the nondiagonal coupling terms in Eq. (8) are ignored. Also, each state is described approximately by a single term in Eq. (7). Despite this truncation, the adiabatic hyperspherical representation includes much of the most important electron correlations. For example, in solving Eq. (6) for the angle functions ϕ_μ and the radial potentials $U_\mu(R)$, ϕ_μ is expanded in coupled pairs of one-electron orbital angular momentum states for the two electrons. Thus, the $^1S^e$ ground state is expanded in ss, pp, dd, and ff pairs. The major advantage of the adiabatic hyperspherical method is that much of the key physics governing physical processes involving two-electron systems is immediately recognizable from the behavior of the adiabatic radial potentials, $U_\mu(R)$, which determine the two-electron radial wave function, $F_\mu(R)$, according to the (truncated) Eq. (8).

In our calculations, we have made a further semiempirical adjustment to the adiabatic hyperspherical ground state energy of the H^- ion. The adiabatic hyperspherical prediction [including the effect of the diagonal coupling term in Eq. (8)] for the ground-state energy is -0.52592 (upper bound). The "exact" nonrelativistic variational result of Pekeris [24] is -0.527751 a.u. The small 0.35% difference between these energies would appear to be negligible. However, the electron affinities of $+0.02592$ a.u. and $+0.027751$ a.u., respectively, differ by 6.6%. While for single-photon detachment this difference is not very important, for multiphoton detachment processes it can lead to serious quantitative errors in the predicted cross sections. This electron affinity difference affects not only the threshold photon frequency at which dissociation can occur, but also affects the radial extent of the ground-state wave function and, hence, the magnitude of the radial transition matrix elements. A quantitative estimate of the effect of electron affinity errors on the N -photon detachment cross sections is derived in Sec. III. Because these errors turn out to be large for the two- and three-photon detachment cross sections we wish to calculate, our $^1S^e$ adiabatic radial potential $U_{\mu=0}(R)$ has been semiempirically adjusted so that the calculated radial ground-state wave function corresponds to the Pekeris [24] value of the H^- ground-state energy.

B. Variationally stable procedure for two-photon detachment

The transition amplitude for a two-photon transition from an initial state $|i\rangle$ to a final state $\langle f|$ is

$$t_{fi}^{(2)} = \left\langle f \left| D \frac{1}{E_i + \omega - H} D \right| i \right\rangle \quad (9)$$

where for light characterized by the polarization vector $\hat{\epsilon}$, the electric dipole operator is given by

$$D \equiv \hat{\epsilon} \cdot \sum_{i=1}^2 \mathbf{r}_i, \quad (10)$$

and where the atomic Hamiltonian H is defined in Eq. (3).

Equation (9) can be cast in a variationally stable form as [18]

$$t_{fi}^{(2)}(\lambda, \lambda') = \langle f | D | \lambda \rangle + \langle \lambda' | D | i \rangle - \langle \lambda' | (E_i + \omega - H) | \lambda \rangle \quad (11)$$

where

$$|\lambda\rangle \equiv \frac{1}{E_i + \omega - H} D | i \rangle, \quad (12)$$

$$\langle \lambda' | \equiv \langle f | D \frac{1}{E_i + \omega - H}. \quad (13)$$

Equation (11) is variationally stable in the sense that any errors in the determination of $|\lambda\rangle$ and $\langle \lambda' |$ enter Eq. (11) only as quadratic and higher powers; no linear terms in these errors appear [18].

In order to evaluate the transition amplitude in Eq. (11), we express the initial, final, and intermediate states as adiabatic hyperspherical wave functions:

$$|i\rangle = \left(R^{5/2} \sin \alpha \cos \alpha \right)^{-1} F_{\mu_i}(R) \phi_{\mu_i}, \quad (14)$$

$$|f\rangle = \left(R^{5/2} \sin \alpha \cos \alpha \right)^{-1} F_{\mu_f}(R) \phi_{\mu_f}, \quad (15)$$

$$|\lambda\rangle = \left(R^{5/2} \sin \alpha \cos \alpha \right)^{-1} \lambda_\mu(R) \phi_\mu, \quad (16)$$

$$\langle \lambda' | = \left(R^{5/2} \sin \alpha \cos \alpha \right)^{-1} \lambda'_\mu(R) \phi_\mu. \quad (17)$$

In our calculations μ_i denotes the lowest $^1S^e$ adiabatic hyperspherical channel, μ denotes the lowest $^1P^o$ channel, and μ_f denotes either the lowest $^1S^e$ or the lowest $^1D^e$ channel.

The first two matrix elements in Eq. (11) thus become

$$\langle \lambda' | d | i \rangle = \int_0^\infty I_{\mu\mu_i}^L(R) \lambda'_\mu(R) R F_{\mu_i}(R) dR, \quad (18)$$

$$\langle f | D | \lambda \rangle = \int_0^\infty I_{\mu_f\mu}^L(R) F_{\mu_f}(R) R \lambda_\mu(R) dR, \quad (19)$$

where $I_{\mu'\mu}^L(R)$, which has been given explicitly by Park *et al.* [27], comes from the integration over the angles $\hat{\mathbf{r}}_1, \hat{\mathbf{r}}_2$, and α using the length (L) form of the electric-dipole operator D . The third matrix element in Eq. (11) is given by

$$\langle \lambda' | E_i + \omega - H | \lambda \rangle = \langle \lambda'_\mu(R) | E_i + \omega - h_\mu^{\text{ad}}(R) | \lambda_\mu(R) \rangle, \quad (20)$$

where

$$h_{\mu}^{\text{ad}}(R) \equiv -\frac{1}{2} \left[\frac{d^2}{dR^2} + \frac{U_{\mu}(R) + 1/4}{r^2} + \left(\phi_{\mu}, \frac{\partial^2}{\partial R^2} \phi_{\mu} \right) \right]. \quad (21)$$

Our numerical procedure for calculating the two-photon transition amplitude is, finally, as follows. Equations (18)–(20) are substituted in Eq. (11). The unknown radial functions $\lambda_{\mu}(R)$ and $\lambda'_{\mu}(R)$ are each expanded in an L^2 basis set of Slater orbitals. The coefficients of this expansion are determined by requiring that Eq. (11) be variationally stable [18]. This procedure is to be contrasted with the adiabatic hyperspherical calculation of Fink and Zoller [4]. They calculate the two-photon transition amplitude using Eq. (19) and the Dalgarno-Lewis procedure [28]. Specifically, their radial function $\lambda_{\mu}(R)$ in Eq. (19) is calculated by solving the inhomogeneous radial equation that results from operating from the left on Eq. (12) with $(E_i + \omega - H)$ and integrating over all angular coordinates.

C. Variationally stable procedure for three-photon detachment

The adiabatic hyperspherical approximation to the three-photon transition amplitude may be expressed in terms of the radial functions defined above as the following radial matrix element:

$$t_{fi}^{(3)} = \sum_{\mu_2, \mu_1} \langle F_{\mu_f} | I_{\mu_f \mu_2}^L(R) R (E_i + 2\omega - h_{\mu_2}^{\text{ad}})^{-1} \\ \times I_{\mu_2 \mu_1}^L(R) R (E_i + \omega - h_{\mu_1}^{\text{ad}})^{-1} \\ \times I_{\mu_1 \mu_i}^L(R) R | F_{\mu_i} \rangle. \quad (22)$$

Here the summations extend over all adiabatic hyperspherical channels μ_1, μ_2 converging to the $H(n=1)$ threshold that are permitted by electric-dipole selection rules. Defining $|\lambda_{\mu_2 \mu_1}\rangle$ and $\langle \lambda'_{\mu_2 \mu_1}|$ as

$$|\lambda_{\mu_2 \mu_1}\rangle \equiv (E_i + 2\omega - h_{\mu_2}^{\text{ad}})^{-1} I_{\mu_2 \mu_1}^L(R) R \\ \times (E_i + \omega - h_{\mu_1}^{\text{ad}})^{-1} I_{\mu_1 \mu_i}^L(R) R | F_{\mu_i} \rangle \quad (23)$$

$$\langle \lambda'_{\mu_2 \mu_1}| \equiv \langle F_{\mu_f} | I_{\mu_f \mu_2}^L(R) R (E_i + 2\omega - h_{\mu_2}^{\text{ad}})^{-1} \\ \times I_{\mu_2 \mu_1}^L(R) R (E_i + \omega - h_{\mu_1}^{\text{ad}})^{-1}, \quad (24)$$

the transition amplitude in Eq. (22) may be written in the following variationally stable form [18, 19]:

$$t_{fi}^{(3)} = \sum_{\mu_2, \mu_1} \langle F_{\mu_f} | I_{\mu_f \mu_2}^L(R) R |\lambda_{\mu_2 \mu_1}\rangle \\ + \sum_{\mu_2, \mu_1} \langle \lambda'_{\mu_2 \mu_1}| I_{\mu_1 \mu_i}^L(R) R | F_{\mu_i} \rangle \\ - \sum_{\mu_2, \mu_1} \langle \lambda'_{\mu_2 \mu_1}| (E_i + \omega - h_{\mu_1}^{\text{ad}}) [I_{\mu_2 \mu_1}^L(R) R]^{-1} \\ \times (E_i + 2\omega - h_{\mu_2}^{\text{ad}}) |\lambda_{\mu_2 \mu_1}\rangle. \quad (25)$$

In our calculations for three-photon detachment, μ_f denotes either the lowest ${}^1F^o$ channel or, for the case of

linearly polarized light only, the lowest ${}^1P^o$ channel; μ_2 denotes either the lowest ${}^1D^e$ channel or, for the case of linearly polarized light only, the lowest ${}^1S^e$ channel; finally, μ_1 denotes the lowest ${}^1P^o$ channel. These lowest channels all converge to the $H(n=1)$ threshold. In principle, one can add higher channels having the same symmetries but converging to the $H(n=2)$ and higher thresholds. However, we have found the higher adiabatic hyperspherical channels are not needed to obtain accurate results.

Note that, for each pair of intermediate channels (μ_2, μ_1) contributing to the three-photon transition amplitude in Eq. (25), the form of their contribution is very similar to the variationally stable form for the two-photon transition amplitude [cf. Eq. (11)]. Only the third term is different. We evaluate the three-photon transition amplitude in Eq. (25) by expanding each $\lambda_{\mu_2 \mu_1}$, and $\lambda'_{\mu_2 \mu_1}$ function in an L^2 basis of Slater orbitals and requiring the coefficients of the expansions to satisfy the variational stability conditions for Eq. (25).

III. ANALYTIC ZERO-RANGE POTENTIAL MODEL FORMULAS FOR MULTIPHOTON DETACHMENT CROSS SECTIONS

We present here analytic expressions for multiphoton detachment cross sections in the approximations that, first, the detached electron may be represented by a plane wave and, second, that the initial state may be represented by a zero-range potential-model wave function. These formulas are presented primarily in order to estimate the sensitivity of theoretical multiphoton detachment cross section results to any inaccuracies in the value of the negative ion's electron affinity. As we shall show, even for the two- and three-photon processes treated here, the theoretical cross sections are very sensitive to the value of the electron affinity employed. We have verified this sensitivity numerically in our adiabatic hyperspherical calculations, as discussed in Sec. V below. Regarding the zero-range potential model, Geltman [16(b)] has presented a recurrence relation for the N -photon transition amplitude. We present here explicit expressions for the N -photon detachment cross sections in the case of circularly polarized light and for the $N=1, 2,$ and 3 photon detachment cross sections in the case of linearly polarized light.

A. Free-electron approximation results

If we assume that the bound electron is described by the wave function $\psi_i(\mathbf{r})$, that the detached electron is described by the plane wave,

$$\psi_f(\mathbf{r}) = (2\pi)^{-3/2} e^{i\mathbf{k}_f \cdot \mathbf{r}}, \quad (26)$$

and that the electric field of the incident light is described by

$$\mathbf{E} = E_0 \hat{\mathbf{e}} \sin \omega t, \quad (27)$$

then the time-independent transition amplitude for N -photon detachment in lowest-order perturbation theory is

$$T_{fi}^{(N)} = \lim_{\eta \rightarrow 0} \frac{1}{2} \left(\frac{-E_0}{i} \right)^N \left\langle (2\pi)^{3/2} e^{i\mathbf{k}_f \cdot \mathbf{r}} \left| \hat{\mathbf{e}} \cdot \mathbf{r} \frac{1}{k_{N-1}^2 + \nabla^2 + i\eta} \hat{\mathbf{e}} \cdot \mathbf{r} \frac{1}{k_{N-2}^2 + \nabla^2 + i\eta} \right. \right. \\ \left. \left. \times \cdots \hat{\mathbf{e}} \cdot \mathbf{r} \frac{1}{k_1^2 + \nabla^2 + i\eta} \hat{\mathbf{e}} \cdot \mathbf{r} \left| \psi_i(\mathbf{r}) \right. \right\rangle, \quad (28)$$

where

$$\frac{1}{2} k_n^2 = E_i + n\omega \quad (29a)$$

and

$$\frac{1}{2} k_f^2 = E_i + N\omega. \quad (29b)$$

(Note that the transition operators $t_{fi}^{(2)}$ and $t_{fi}^{(3)}$ defined in Eqs. (9) and (22) are formally related to $T_{fi}^{(N)}$ in Eq. (28) by the relation

$$T_{fi}^{(N)} = \left(-\frac{E_0}{2i} \right)^N t_{fi}^{(N)} \quad (30)$$

due to the fact that only the polarization vector of the electric field was used to define $t_{fi}^{(N)}$ [cf. Eqs. (10) and (27)]. Of course the wave functions used to calculate each amplitude are quite different; thus the equality in Eq. (30) holds only when the same wave functions are used to calculate each amplitude.) By expressing the initial state ψ_i in terms of its Fourier transform, $\phi_i(\mathbf{k})$,

$$\psi_i(\mathbf{r}) \equiv (2\pi)^{-3/2} \int d^3\mathbf{k} \phi_i(\mathbf{k}) e^{i\mathbf{k} \cdot \mathbf{r}}, \quad (31)$$

$$\hat{\mathbf{e}} \cdot \nabla_{\mathbf{k}} f(k) Y_{\ell m}(\hat{\mathbf{k}}) = \left[(-1)^{\ell' - m'} (\ell')^{1/2} \begin{pmatrix} \ell' & 1 & \ell \\ -m' & q & m \end{pmatrix} Y_{\ell' m'} \left(\frac{d}{dk} - \frac{\ell}{k} \right) f(k) \right]_{\substack{\ell' = \ell + 1 \\ m' = m + q}} \\ + \left[(-1)^{\ell - m'} (\ell)^{1/2} \begin{pmatrix} \ell' & 1 & \ell \\ -m' & q & m \end{pmatrix} Y_{\ell' m'} \left(\frac{d}{dk} + \frac{(\ell + 1)}{k} \right) f(k) \right]_{\substack{\ell' = \ell - 1 \\ m' = m + q}}. \quad (34)$$

Given the transition amplitude $T_{fi}^{(N)}$, the transition rate is given by the golden rule as

$$\frac{dW_{fi}^{(N)}}{d\Omega_{\mathbf{k}_f}} = 2\pi |T_{fi}^{(N)}|_{k=k_f}^2 k_f, \quad (35)$$

and for an incident photon flux ($cE_0^2/8\pi\omega$) the total N -photon detachment cross section is given by

$$\sigma_{fi}^{(N)} = \frac{8\pi\omega}{cE_0^2} \int \frac{dW_{fi}^{(N)}}{d\Omega_{\mathbf{k}_f}} d\Omega_{\mathbf{k}_f}. \quad (36)$$

B. Zero-range potential model results

In order to evaluate the N -photon transition amplitude in Eq. (32) using the gradient formula in Eq. (34) we require a specific form for the momentum-space wave function, $\phi_i(\mathbf{k})$, of the initial state. We choose

$$\phi_i(\mathbf{k}) \equiv 2^{3/2} B (k^2 - 2E_i)^{-1} Y_{00}(\hat{\mathbf{k}}), \quad (37)$$

and inserting complete sets of plane wave states between each of the operators in Eq. (28), we obtain the momentum space expression for $T_{fi}^{(N)}$:

$$T_{fi}^{(N)} = \frac{1}{2} (-E_0)^N \left[\hat{\mathbf{e}} \cdot \nabla_{\mathbf{k}} \frac{1}{k_{N-1}^2 - k^2} \hat{\mathbf{e}} \cdot \nabla_{\mathbf{k}} \frac{1}{k_{N-2}^2 - k^2} \right. \\ \left. \times \cdots \hat{\mathbf{e}} \cdot \nabla_{\mathbf{k}} \frac{1}{k_1^2 - k^2} \hat{\mathbf{e}} \cdot \nabla_{\mathbf{k}} \phi_i(\mathbf{k}) \right]_{k=k_f}. \quad (32)$$

In deriving Eq. (32), we have used the result

$$\langle (2\pi)^{-3/2} e^{i\mathbf{k}' \cdot \mathbf{r}} | \hat{\mathbf{e}} \cdot \mathbf{r} | (2\pi)^{-3/2} e^{i\mathbf{k} \cdot \mathbf{r}} \rangle \\ = -i \hat{\mathbf{e}} \cdot \nabla_{\mathbf{k}} \delta(\mathbf{k} - \mathbf{k}') \quad (33)$$

as well as the fact that the imaginary parts in Eq. (28) do not contribute to Eq. (32) since for $k = k_f$, none of the energy denominators in Eq. (32) is singular.

One may proceed to evaluate the transition amplitudes in Eq. (32) by using the gradient formula [29]:

where B is a normalization constant. This form of the initial-state wave function is a well-known approximation stemming from the effective range theory for an s electron [30]. It represents also the solution of an attractive spherical δ -function potential, whose effect may be described by a particular boundary condition at the origin [31].

For H^- the constant B in Eq. (37) is properly chosen to have the value 0.315 52, as explained in detail by Du and Delos [32]. Briefly, we note that this is not the value which normalizes the approximate ground-state wave function. Rather B is the constant which normalizes the exact ground-state wave function according to the effective range theory [30], i.e.,

$$B^2 = (k_b/2\pi)(1 - k_b r_{\text{eff}})^{-1}, \quad (38)$$

where

$$k_b^2/2 \equiv |E_i|. \quad (39)$$

Its value for H^- is obtained from the variational calculation of Ohmura and Ohmura [33], who found that

$$k_b = 0.235\,588\,3, \quad (40a)$$

and

$$\tau_{\text{eff}} = 2.646. \quad (40b)$$

Substituting the ground-state wave function in Eq. (37) into Eq. (32) for the N -photon transition amplitude and using Eqs. (34)–(36), we find the following analytic expressions for the N -photon detachment cross sections $\sigma_{fi}^{(N)}(L)$ and $\sigma_{fi}^{(N)}(C)$ for the cases of linearly (L) and circularly (C) polarized incident light of frequency ω :

$$\sigma_{fi}^{(N=1)}(L) = \left(\frac{2^3 \pi^2 B^2}{3c} \right) \left(\frac{k_f^3}{\omega^3} \right), \quad (41)$$

$$\sigma_{fi}^{(N=2)}(L) = \left(\frac{\pi^2 B^2 E_0^2}{2c} \right) \left(\frac{\frac{1}{5} k_f^5 - \frac{1}{3} \omega k_f^3 + \frac{1}{4} \omega^2 k_f}{\omega^7} \right), \quad (42)$$

$$\sigma_{fi}^{(N=3)}(L) = \left(\frac{\pi^2 B^2 E_0^4}{2^3 3^2 c} \right) \left(\frac{\frac{1}{7} k_f^7 - \frac{3}{5} \omega k_f^5 + \frac{3}{4} \omega^2 k_f^3}{\omega^{11}} \right), \quad (43)$$

$$\sigma_{fi}^{(N)}(C) = \left[\frac{(2N)!! \pi^2 B^2 E_0^{2N-2}}{2^{3N-5} (N!)^2 (2N+1)!! c} \right] \left(\frac{k_f^{2N+1}}{\omega^{4N-1}} \right), \quad (44)$$

where k_f is related to ω in each case according to Eq. (29b). We note that, as may be expected, these results are identical to those obtained by using a Volkov final-state wave function to calculate the N -photon detachment cross sections nonperturbatively and then taking the weak laser field limit (i.e., $E_0 \rightarrow 0$) of the resulting formulas [34].

C. Sensitivity of the N -photon detachment cross sections to the electron affinity

We proceed here to estimate the fractional error to be expected in theoretical calculations of N -photon detachment cross sections if the value of the electron affinity ($-E_i$) for the negative ion [cf. Eq. (29b)] is in error by the amount $-\Delta E_i$. For a calculation of $\sigma^{(N)}$ at the detached electron kinetic energy $\frac{1}{2}k_f^2$, the fractional error in the photon frequency is

$$\frac{\Delta\omega}{\omega} \equiv \frac{-\Delta E_i}{\frac{1}{2}k_f^2 - E_i}. \quad (45)$$

If in a theoretical calculation one uses an approximate photon frequency ω_a based on the incorrect electron affinity $-(E_i + \Delta E_i)$, then we may write

$$\omega_a = \omega \left(1 + \frac{\Delta\omega}{\omega} \right). \quad (46)$$

One sees readily from substitution of Eq. (46) in Eq. (44) that the fractional error in the N -photon detachment cross section for circularly polarized light is

$$\frac{\Delta\sigma^{(N)}(C)}{\sigma^{(N)}(C)} \approx (4N-1) \left(\frac{-\Delta\omega}{\omega} \right). \quad (47)$$

Since in most cases $\Delta\omega$ is negative, this implies that as N increases the theoretically predicted N -photon dissociation cross section will be increasingly too large.

The case of $\sigma^{(N)}(L)$ for linearly polarized light requires a more careful analysis. For this analysis we have examined the low-intensity limit of the nonperturbative N -photon detachment cross sections calculated assuming the detached electron may be represented by a Volkov state [34]. However, the results may be understood as a simple extrapolation in N of the formulas for $N = 1 - 3$ given in Eqs. (41)–(43).

Far above threshold, i.e., $\frac{1}{2}k_f^2 \gg |E_i|$, the error in the magnitude of $\sigma^{(N)}(L)$ is determined by the term having the highest power of k_f , particularly for large values of N . One finds then that

$$\sigma^{(N)}(L) \underset{k_f \rightarrow \infty}{\sim} C_1 \frac{k_f^{2N+1}}{\omega^{4N-1}}, \quad (48)$$

where C_1 is a constant. For this high-energy limit, then, the fractional error in $\sigma^{(N)}(L)$ is the same as for $\sigma^{(N)}(C)$ and is given by Eq. (47).

Near threshold, i.e., $\frac{1}{2}k_f^2 \ll |E_i|$, the error in the magnitude of $\sigma^{(N)}(L)$ is determined by the term having the highest power of ω in the numerator of the fraction shown for $N = 1 - 3$ in Eqs. (41)–(43). In this limit one finds

$$\sigma^{(N)}(L) \underset{k_f \rightarrow 0}{\rightarrow} \begin{cases} C_2 \frac{k_f}{\omega^{3N-1}} & (N = \text{even}) \\ C_3 \frac{k_f^3}{\omega^{3N}} & (N = \text{odd}), \end{cases} \quad (49a)$$

where C_2 and C_3 are constants. Accordingly the fractional error in the linear polarization cross section near threshold is estimated as

$$\frac{\Delta\sigma^{(N)}(L)}{\sigma^{(N)}(L)} \underset{k_f \rightarrow 0}{\rightarrow} \begin{cases} (3N-1) \left(\frac{-\Delta\omega}{\omega} \right) & (N = \text{even}) \\ 3N \left(\frac{-\Delta\omega}{\omega} \right) & (N = \text{odd}). \end{cases} \quad (50a)$$

As we shall show in Sec. V, adiabatic hyperspherical calculations carried out with the adiabatic hyperspherical value of the electron affinity give multiphoton detachment cross sections that are much larger than those obtained in our semiempirical adiabatic hyperspherical calculations. In the latter calculations, the adiabatic hyperspherical potentials are semiempirically adjusted to give the correct electron affinity. The differences in the magnitudes of the multiphoton detachment cross sections are in line with the estimates provided here based on the zero-range potential model.

IV. EFFECT OF FINAL STATE s -WAVE PHASE SHIFTS ON THE TWO-PHOTON DETACHMENT CROSS SECTIONS

Geltman [16(b)] has shown that zero-range potential-model results may be improved significantly by represent-

ing the detached electron with phase-shifted plane waves. This is particularly true for two-photon detachment using linearly polarized light since in that case the dominant partial wave near threshold is the s wave, which has a large overlap with the residual H atom. Geltman obtained his so-called "best phase" results numerically. In order to demonstrate the sensitivity of the two-photon detachment cross section to the s -wave phase shift, we present here analytic expressions for this cross section. Our results show in particular that a necessary condition for the imaginary part of the transition amplitude in Eq. (28) to be nonzero is that the final-state partial waves have nonzero phase shifts.

A. Formulation

We treat here two-photon detachment of an electron bound in a zero-range potential. We use the same initial-state wave function as in Sec. III B. From Eqs. (31) and (37) this is

$$\psi_i(\mathbf{r}) = B \frac{e^{-k_b r}}{r} \equiv \frac{u_0(r)}{r} Y_{00}(\hat{\mathbf{r}}), \quad (51a)$$

where

$$u_0(r) \equiv (4\pi)^{1/2} B e^{-k_b r}, \quad (51b)$$

and where B and k_b are defined in Eqs. (38) and (39) and the immediately following text. Electric-dipole selection rules for detachment of this $\ell = 0$ electron result in only $\ell = 0$ and $\ell = 2$ final-state angular momenta. The energy-normalized radial wave functions for these final states are

$$u_{\ell_f=0}(r) = \left(\frac{2}{\pi k_f} \right)^{1/2} \sin[k_f r + \delta_s(k_f)], \quad (52a)$$

$$u_{\ell_f=2}(r) = \left(\frac{2}{\pi k_f} \right)^{1/2} k_f r j_2(k_f r), \quad (52b)$$

where effective range theory [35] gives the following formula for the s -wave phase shift $\delta_s(k_f)$:

$$k_f \cot \delta_s(k_f) = -k_b + \frac{1}{2} r_{\text{eff}} (k_b^2 + k_f^2), \quad (53)$$

where the variationally determined [33] values of k_b and r_{eff} for the H^- ion are given in Eq. (40).

Treating this short-range potential-model approximation to the H^- ion as a one-electron system and carrying

out the angular integrations by standard procedures for the case of linearly polarized light, we find that the absolute squares of the transition amplitudes to each of the two final states in Eq. (52) are

$$|T_{\ell_f=2}^{(2)}|^2 = \left(\frac{E_0}{2} \right)^4 \left(\frac{4}{45} \right) |P_{\ell_f=2}|^2, \quad (54a)$$

$$|T_{\ell_f=0}^{(2)}|^2 = \left(\frac{E_0}{2} \right)^4 \left(\frac{1}{9} \right) |P_{\ell_f=0}|^2, \quad (54b)$$

where the radial transition amplitude P_{ℓ_f} is defined by

$$P_{\ell_f} \equiv \lim_{\eta \rightarrow 0} \langle u_{\ell_f} | r (E_i + \omega - h_{\ell=1} + i\eta)^{-1} r | u_0 \rangle, \quad (55)$$

where $h_{\ell}(r)$ denotes the radial Hamiltonian for an electron having orbital angular momentum ℓ ,

$$h_{\ell} \equiv -\frac{1}{2} \frac{d^2}{dr^2} + \frac{\ell(\ell+1)}{2r^2}. \quad (56)$$

Substituting Eq. (54) into Eqs. (35) and (36) and taking into account that the final states in Eq. (52) are energy normalized (in contrast to the momentum-normalized plane waves used in Sec. III) we obtain for the two-photon total cross section (in a.u.)

$$\sigma^{(2)} = \frac{\pi^2 \omega}{c} E_0^2 \left[\frac{4}{45} |P_2|^2 + \frac{1}{9} |P_0|^2 \right]. \quad (57)$$

B. Evaluation of the radial transition amplitudes

We evaluate the radial amplitudes in Eq. (55) using the analytic Green's function [36]:

$$\begin{aligned} G_{\ell=1}^{(+)}(r, r') &\equiv \lim_{\eta \rightarrow 0} (E_i + \omega - h_{\ell=1} + i\eta)^{-1} \\ &= -2i k_I r < j_1(k_I r <) r > h_1^{(1)}(k_I r >), \end{aligned} \quad (58)$$

where

$$\frac{1}{2} k_I^2 \equiv E_i + \omega, \quad (59)$$

and where $j_1(k_I r)$ and $h_1^{(1)}(k_I r)$ are spherical Bessel functions of the first and third kinds [37]. Substituting Eq. (58) into Eq. (55) and using Eqs. (51b) and (52) for the initial and final wave functions, we may write the two desired radial amplitudes as

$$P_{\ell_f=0} = 2B(2/k_f)^{1/2} \langle \sin[k_f r + \delta_s(k_f)] | r | \lambda(E_i + \omega, r) \rangle, \quad (60a)$$

$$P_{\ell_f=2} = 2B(2/k_f)^{1/2} \left\{ \frac{3}{k_f^2} \left\langle r^{-1} \sin k_f r \left| \frac{d}{dr} [r \lambda(E_i + \omega, r)] \right. \right\rangle - \langle \sin k_f r | r | \lambda(E_i + \omega, r) \rangle \right\}, \quad (60b)$$

where we have defined

$$\begin{aligned} \lambda(E_i + \omega, r) &\equiv \lim_{\eta \rightarrow 0} (E_i + \omega - h_1 + i\eta)^{-1} r |e^{-k_b r} \rangle \quad (61a) \\ &= -2ik_I r h_1^{(1)}(k_I r) \int_0^r (r')^2 j_1(k_I r') e^{-k_b r'} dr' \\ &\quad - 2ik_I r j_1(k_I r) \int_r^\infty (r')^2 h_1^{(1)}(k_I r') e^{-k_b r'} dr'. \end{aligned} \quad (61b)$$

[Note that in Eq. (60b), the first term in curly brackets results from an integration by parts.]

The analytic form for $\lambda(E_i + \omega, r)$ may be obtained from Eq. (61b). One substitutes the explicit forms for the spherical Bessel functions and then carries out the integrations over r' . The result is

$$\begin{aligned} \lambda(E_i + \omega, r) &= \frac{1}{\omega^2} \left(ik_I - \frac{1}{r} \right) e^{ik_I r} \\ &\quad + \frac{1}{\omega^2} \left(\omega r + k_b + \frac{1}{r} \right) e^{-k_b r}. \end{aligned} \quad (62)$$

The analytic forms for the radial transition amplitudes P_{ℓ_f} in Eq. (60) are obtained by substituting Eq. (62) into Eq. (60) and carrying out the radial integrals. The results are

$$\begin{aligned} P_{\ell_f=0} &= B(2/k_f)^{1/2} (2\omega^2)^{-2} \\ &\quad \times \left\{ (2k_f^3 - 3k_f \omega) \cos[\delta_s(k_f)] \right. \\ &\quad \left. + (5\omega k_b - 2k_b k_f^2 - 4ik_f^3) \sin[\delta_s(k_f)] \right\}, \end{aligned} \quad (63)$$

$$P_{\ell_f=2} = -B(2/k_f)^{1/2} \left(\frac{k_f^3}{2\omega^4} \right). \quad (64)$$

Notice that for $E_i + \omega < 0$, $k_I \equiv \sqrt{2(E_i + \omega)} = i|k_I|$, so that the $-4ik_f^3$ coefficient of the $\sin[\delta_s(k_f)]$ term in the curly braces in Eq. (63) becomes real and equal to $-4|k_I|^3$. For $E_i + \omega > 0$, however, $k_I \equiv |k_I|$ and this coefficient of the $\sin[\delta_s(k_f)]$ term in curly braces in Eq. (63) is imaginary and equal to $-4i|k_I|^3$. In this latter case, $P_{\ell_f=0}$ has a complex value unless $\delta_s(k_f) = 0$, whereupon $P_{\ell_f=0}$ is real. Hence in the free-electron case, $P_{\ell_f=0}$ has no contribution from the energy shell.

The two-photon cross section can now be obtained analytically by substituting the absolute squares of Eqs. (63) and (64) into Eq. (57). The result is

$$\sigma^{(2)} = \sigma_{\ell_f=2}^{(2)} + \sigma_{\ell_f=0}^{(2)}, \quad (65a)$$

where

$$\sigma_{\ell_f=2}^{(2)} = \frac{\pi^2 B^2 E_0^2}{c} \left(\frac{2}{45} \right) \left(\frac{k_f^5}{\omega^7} \right) \quad (65b)$$

and

$$\begin{aligned} \sigma_{\ell_f=0}^{(2)} &= \frac{\pi^2 B^2 E_0^2}{c} (72k_f \omega^7)^{-1} \\ &\quad \times \left| (2k_f^3 - 3k_f \omega) \cos[\delta_s(k_f)] \right. \\ &\quad \left. + (5\omega k_b - 2k_b k_f^2 - 4ik_f^3) \sin[\delta_s(k_f)] \right|^2. \end{aligned} \quad (65c)$$

Note that in the limit $\delta_s(k_f) \rightarrow 0$, Eq. (65) becomes equal to the free-electron result in Eq. (42). In the near-threshold region, the energy-dependent s -wave phase shift $\delta_s(k_f)$ should represent most of the final-state electron-correlation effects, as we shall show by comparison with our semiempirical adiabatic hyperspherical results in the next section.

V. RESULTS

We present here our semiempirical adiabatic hyperspherical results for two- and three-photon detachment of H^- for the cases of linearly and circularly polarized light. In order to elucidate the role of electron correlations in multiphoton detachment of H^- , we compare our results with the free-electron, zero-range potential-model results derived in Sec. III as well as, for the case of two-photon detachment, the phase-shifted zero-range potential-model results derived in Sec. IV. In order to demonstrate the sensitivity of the theoretical results to the electron affinity of H^- , as discussed in Sec. III C, we compare our semiempirical adiabatic hyperspherical predictions with adiabatic hyperspherical predictions. Finally, we compare our results with other calculations which include electron-correlation effects [10,13,14].

A. Numerical aspects

In our variationally stable procedure for evaluating the two- and three-photon transition matrices in Eqs. (11) and (25) respectively, the unknown functions λ and λ' are each expanded in Slater orbital bases. For the case of two-photon detachment, about 70 Slater orbitals were used, each having the same exponential function. For the case of three-photon detachment, a total of about 120 Slater orbitals were used, with two different exponential functions.

In our semiempirical adiabatic hyperspherical treatment, we adjust the adiabatic hyperspherical radial potentials $U_\mu(r)$ in Eq. (8), ignoring the coupling terms, so that the total ground-state energy E_g for H^- agrees with the nonrelativistic energy predicted by Pekeris [24], i.e., -0.527751 a.u. This compares with the adiabatic hyperspherical value of -0.52592 a.u. The adjustment of $U_\mu(R)$ is accomplished by deepening the bottom of the well very slightly and smoothly joining the deepened part onto the adiabatic hyperspherical potential by a spline procedure. No correction to the angular function ϕ_μ for

the $1S$ channel was made. The final-state radial function for the $1S$ detachment channel was also calculated in the semiempirically adjusted radial potential $U_\mu(R)$. Finally, we note that our potentials $U_\mu(R)$ and angle functions ϕ_μ were only calculated numerically for $R \leq 40$ a.u. In the range $40 \text{ a.u.} \leq R \leq 120 \text{ a.u.}$, the analytically known asymptotic forms for these functions [20] were used. A spline fit was used to join the numerical and analytic values of quantities dependent on $U_\mu(R)$ and ϕ_μ in the vicinity of $R \approx 40$ a.u.

We present our results for the generalized cross sections [17], which depend only on the properties of the H^- system and not on the electric field strength E_0 of the incident light. The generalized cross section $\hat{\sigma}^{(N)}$ is defined in terms of the cross sections in Eqs. (36), (41)–(44), (57), and (65) by

$$\hat{\sigma}^{(N)} \equiv \frac{\sigma^{(N)}}{FN-1}, \quad (66a)$$

where the photon flux is

$$F = \frac{E_0^2 c}{8\pi\hbar\omega}. \quad (66b)$$

B. Two-photon detachment of H^-

In Fig. 1 we see that our semiempirical adiabatic hyperspherical result for two-photon detachment of H^- with linearly polarized light is about 25% lower in magnitude than the adiabatic hyperspherical result for $\frac{1}{2}k_f^2 = 0.01$ a.u. Alternatively, the adiabatic hyperspherical result is 33% larger than the semiempirical adiabatic hyperspherical result. This compares well with the analytic zero-range potential-model estimates for the expected error in the calculated cross sections due to the different electron affinities. The Pekeris value [24] for the electron affinity $-E_i$ is $+0.027751$ a.u., while the adiabatic hyperspherical value is $+0.02592$ a.u. At a detached electron

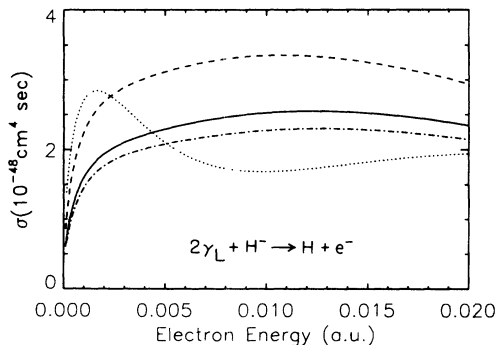


FIG. 1. Generalized cross sections for two-photon detachment of H^- using linearly polarized light plotted vs photoelectron kinetic energy. Solid curve: Semiempirical adiabatic hyperspherical results. Dashed curve: adiabatic hyperspherical results. Dotted curve: free-electron zero-range potential-model results. Dash-dotted curve: Zero-range potential-model results with nonzero, final-state s -wave phase shifts.

kinetic energy $\frac{1}{2}k_f^2 = 0.01$ a.u., this gives a fractional error in the photon energy, according to Eq. (43), of $(\Delta\omega/\omega) = -0.049$. Hence, according to the estimates in Eqs. (48) and (50a), for linearly polarized light the adiabatic hyperspherical cross sections will be in error by from 24% to 34% at this value of k_f , although neither of the limits at which these formulas apply (i.e., $k_f \rightarrow \infty$ and $k_f \rightarrow 0$ respectively) really applies at $\frac{1}{2}k_f^2 = 0.01$ a.u. However, the order of magnitude in the error is quite well predicted.

One sees from Fig. 1 also that the semiempirical adiabatic hyperspherical cross section is about 11% higher at $\frac{1}{2}k_f^2 = 0.01$ a.u. than the zero-range potential model result calculated according to Eq. (65), in which the $\ell_f = 0$ partial wave is phase shifted. We attribute this increase above the phase-shifted zero-range potential-model cross section as due to the electron correlations treated in our semiempirical adiabatic hyperspherical calculation. That electron correlations increase the H^- two-photon detachment cross section has been noted by Crance [13]. This contrasts with electron-correlation effects on the two-photon detachment cross sections of F^- [38] and Cl^- [39], which lower the calculated cross sections relative to Hartree-Fock (HF) predictions. (Of course, it is not clear how the zero-range potential-model predictions compare to results of a HF calculation for H^- .)

The free-electron, zero-range potential-model results shown in Fig. 1 have an incorrect energy dependence above threshold. The cross section peaks near 10^{-3} a.u. electron energy and then rapidly decreases to a minimum value near 10^{-2} a.u., whereupon it rises slowly with increasing electron energy. Note also that our zero-range potential-model predictions are $\approx 30\%$ larger than those of Geltman [16]. This difference stems from our different approaches to the zero-range potential model [40]. Geltman [16] treats H^- as a two-electron system whose $1s$ orbital in both initial and final states is the zero-range potential-model wave function, normalized to unity. We treat H^- as a one-electron system in which the initial-state wave function is the zero-range potential-model wave function, normalized according to effective range theory (cf. Sec. III B).

In Fig. 2 we compare our semiempirical adiabatic hyperspherical result with other theoretical results that include electron correlations: the correlated basis calculation of Crance [13], the initial-state correlation results (using a Hylleraas-type wave function) of Dörr *et al.* [14], and the many-electron, many-photon theory (MEMPT) results of Mercouris and Nicolaides [10(c)]. Our results lie about a factor of 2 higher than those of Crance; also our results rise much more sharply to a broad plateau above threshold. The magnitude of our results is generally in agreement with those of Mercouris and Nicolaides, although their results appear to mimic slightly the near-threshold peak and subsequent decreasing cross section of the zero-range potential-model results shown in Fig. 1. The results of Dörr *et al.* show that inclusion of ground-state correlations alone gives a much better description of the near-threshold rise of the cross section than does the zero-range potential model. Their results

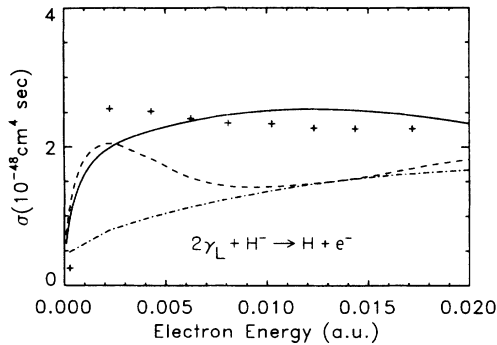


FIG. 2. Generalized cross sections for two-photon detachment of H^- using linearly polarized light plotted vs photoelectron kinetic energy. Solid curve: present semiempirical adiabatic hyperspherical results. Pluses: MEMPT results of Mercouris and Nicolaides [10(c)]. Dashed curve: Correlated ground state calculation of Dörr *et al.* [14]. Dash-dotted curve: correlated-basis calculation of Crance [13].

are very close to ours from threshold to about 0.0015 a.u. above. Further above threshold, however, their use of a free-electron final state results in their cross section mimicking the shape of the free-electron zero-range potential-model cross section.

In Fig. 3 we present the generalized cross section for two-photon detachment of H^- with circularly polarized light. We see that at $\frac{1}{2}k_f^2 = 0.02$ a.u., the adiabatic hyperspherical results are $\approx 28\%$ larger than our semiempirically adjusted adiabatic hyperspherical results. This compares very well with the zero-range potential-model estimate of 27% given by Eq. (47). Our semiempirical adiabatic hyperspherical results are $\approx 9\%$ larger than predictions of the free-electron zero-range potential model. As for the case of linearly polarized light, we attribute this difference to electron-correlation effects. The energy dependence of our semiempirical adiabatic hyperspherical results appears to be consistent with that predicted by Dörr *et al.* [14], however our results have a magnitude approximately three times larger.

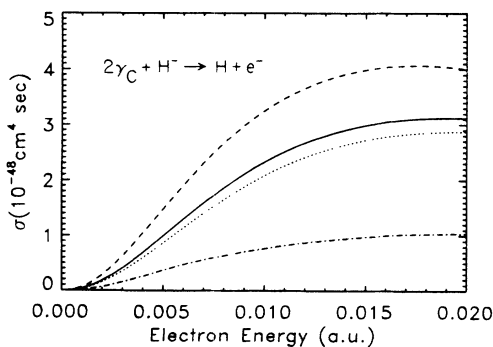


FIG. 3. Generalized cross sections for two-photon detachment of H^- using circularly polarized light plotted vs photoelectron kinetic energy. Solid, dashed, and dotted curves have the same connotation as in Fig. 1. Dash-dotted curve: correlated ground-state calculation of Dörr *et al.* [14].

C. Three-photon detachment of H^-

In Fig. 4 we present our generalized cross sections for three-photon detachment of H^- using linearly polarized light. At the maximum in the cross section near $\frac{1}{2}k_f^2 = 0.003$ a.u., the adiabatic hyperspherical result is $\approx 67\%$ greater than the semiempirical adiabatic hyperspherical result. At this kinetic energy, $\Delta\omega/\omega = -0.06$, so that the zero-range potential-model estimates for the difference between the cross sections are $\approx 65\%$ [using Eqs. (48) and (47)] and $\approx 54\%$ [using Eq. (50b)]. Since k_f is neither infinite nor zero, neither of these estimates applies at the cross section maximum. However, the order of magnitude of the error in the adiabatic hyperspherical cross section due to the error in the electron affinity is correctly predicted.

Surprisingly, Fig. 4 shows that our semiempirical adiabatic hyperspherical results are in excellent agreement with predictions of the free-electron zero-range potential model from threshold to the region of the cross section maximum. At higher energies, our semiempirical adiabatic hyperspherical results decrease faster than those of the free-electron zero-range potential model. In this latter model, the $\ell_f = 1$ and $\ell_f = 3$ partial waves of the detached electron are not phase shifted. However, the phase shifts for these partial waves are in any case small [16(b)]. Note that our zero-range potential-model results are $\approx 30\%$ larger at the cross section maximum than the zero-range potential-model results of Geltman [16]. As noted above, this difference stems from our different approaches to the zero-range potential model [40]. Geltman [16] treats H^- as a two-electron system whose $1s$ orbital in both initial and final states is the zero-range potential-model wave function, normalized to unity. We treat H^- as a one-electron system in which the initial-state wave function is the zero-range potential-model wave function, normalized according to effective range theory (cf. Sec. III B).

Our semiempirical adiabatic hyperspherical results differ significantly from those of other calculations which

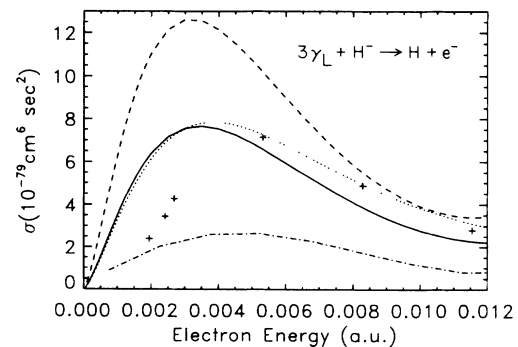


FIG. 4. Generalized cross section for three-photon detachment of H^- using linearly polarized light plotted vs photoelectron kinetic energy. Solid, dashed, and dotted curves have the same connotation as in Fig. 1. Pluses: MEMPT results of Mercouris and Nicolaides [10(c)]. Dash-dotted curve: Correlated-basis calculation of Crance [13].

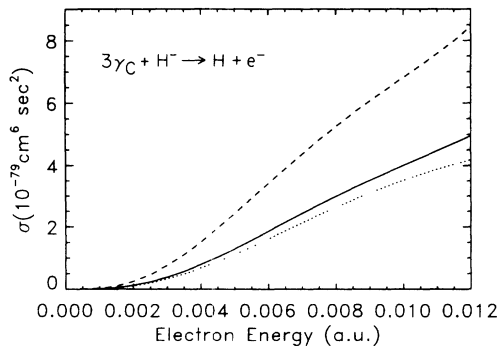


FIG. 5. Generalized cross section for three-photon detachment of H^- using circularly polarized light plotted vs photoelectron kinetic energy. Solid, dashed, and dotted curves have the same connotation as in Fig. 1.

include electron-correlation effects. As shown in Fig. 4, below the cross section maximum our results are a factor of 2 or so larger than those of Mercouris and Nicolaides [10(c)]. Above the maximum, our results are in much closer agreement with theirs, although their results agree best with our free-electron zero-range potential-model results. In contrast, over the entire energy region shown our results lie a factor of 3 or so larger than those of Crance [13].

Finally, in Fig. 5 we present our generalized cross section results for three-photon detachment of H^- using circularly polarized light. At the highest energy shown, $\frac{1}{2}k_f^2 = 0.012$ a.u., the adiabatic hyperspherical result lies 70% higher than our semiempirical adiabatic hyperspherical result. This compares reasonably with the zero-range potential-model estimate for the difference in the cross sections (based on the different electron affinities) of 51%, which was obtained from Eq. (47). Over the entire energy range shown, the semiempirical adiabatic hyperspherical results are close to those of our free-electron zero-range potential model. This indicates the rather small effect of electron correlations on the cross sections for circularly polarized light.

VI. CONCLUSIONS

In this paper we have examined the role of many-body effects on multiphoton detachment of the fundamental H^- ion. We have compared results of a two-electron semiempirical adiabatic hyperspherical calculation with results of two single-electron, zero-range potential-model calculations: one in which the detached electron is described by a plane wave and one (for the case of two-photon detachment using linearly polarized light) in which the detached electron's $\ell_f = 0$ partial wave is phase shifted. We find that for two-photon detachment using linearly polarized light the use of the s -wave final-state phase shift in the zero-range potential-model calculation is crucial to obtain reasonable agreement with the more accurate semiempirical, adiabatic hyperspherical results. For the other cases considered, two- and three-photon detachment with circularly polarized light

as well as three-photon detachment with linearly polarized light, the free-electron zero-range potential-model predictions are reasonably close to the predictions of the more accurate hyperspherical results, especially for circularly polarized light.

It should be noted that it is difficult to quantify precisely the role of electron correlations on multiphoton cross sections for H^- . Since H^- is not bound in Hartree-Fock approximation, we cannot use the standard measure of electron correlation, namely, the difference between a HF result and the corresponding result of a treatment which goes beyond the HF approximation by including interactions not treated in the HF approximation. In this paper we have therefore put forward the comparison of our semiempirical adiabatic hyperspherical results with results of single-electron model calculations as indicative of the magnitude of effects due to electron correlations.

We have presented analytic formulas for our zero-range potential-model cross sections. These have been used to predict a significant sensitivity of the theoretical cross sections to the value of the electron affinity used in the theoretical calculations. This sensitivity has been demonstrated numerically by comparing results of two adiabatic hyperspherical calculations: one using the adiabatic hyperspherical value of the electron affinity and one semiempirically adjusted to give the variationally determined nonrelativistic electron affinity predicted by Pekeris [24].

The sensitivity of the theoretical predictions on the electron affinity may explain perhaps some of the disparity between theoretical predictions of multiphoton detachment cross sections for H^- by different theoretical groups. We have compared our semiempirical adiabatic hyperspherical results with those of three other calculations which include electron correlations. On the whole, our results agree best quantitatively with those of Mercouris and Nicolaides [10(c)], especially away from the near-threshold region. However, near threshold the agreement is not as good as that between our semiempirical adiabatic hyperspherical results and our best zero-range potential-model results (i.e., for two-photon detachment with linearly polarized light, our phase-shifted zero-range potential results, and for all other cases, our free-electron zero-range potential results).

Finally, in the Appendix we have shown that the low-intensity limit of the Keldysh treatment of multiphoton detachment reduces to the perturbative results we present in Sec. III.

ACKNOWLEDGMENTS

AFS gratefully acknowledges discussions and correspondence with M. Crance, S. Geltman, and R. Shakeshaft regarding their related works. He also acknowledges the hospitality of the Joint Institute for Laboratory Astrophysics and partial support from the JILA Visiting Fellowship program. This work was supported in part by the U.S. Department of Energy, Office of Basic Energy Sciences, Division of Chemical Sciences, under Grant No. DE-FG02-88ER13955.

**APPENDIX: LOW-INTENSITY LIMIT
OF KELDYSH-THEORY MULTIPHOTON
DETACHMENT TRANSITION AMPLITUDES**

We derive here the low-intensity limit of Keldysh-theory transition amplitudes for multiphoton detachment. We show that they are equal to the results of perturbation theory in which the detached electron is free and in which the length form of the perturbation is used.

1. Form of the transition amplitude

In the Keldysh approximation, the length gauge is used for describing the interaction of an electron with a laser field. The S matrix in the length gauge is [41]

$$S_{fi}^L = -i \int_{-\infty}^{+\infty} \langle \psi_f^L | V_f^L | \psi_i \rangle dt, \quad (\text{A1})$$

where ψ_i is the initial-state wave function, which is assumed to be unaffected by the laser field; where ψ_f^L is the exact solution for a free electron moving under the influence of the laser-electron interaction V_f^L ; and where V_f^L is given in momentum space by

$$V_f^L = iE_0 \sin \omega t \hat{\mathbf{e}} \cdot \nabla_{\mathbf{p}}, \quad (\text{A2})$$

where the laser electric field is defined by Eq. (27). Using the following properties of the initial- and final-state wave functions,

$$i \frac{\partial}{\partial t} \psi_i = \epsilon_i \psi_i, \quad (\text{A3})$$

$$V_f^L \psi_f^L = \left[i \frac{\partial}{\partial t} - \frac{1}{2} p^2 \right] \psi_f^L, \quad (\text{A4})$$

Eq. (A1) may be rewritten as

$$S_{fi}^L = i \int_{-\infty}^{+\infty} \langle \psi_f^L | \frac{1}{2} p^2 - \epsilon_i | \psi_i \rangle dt. \quad (\text{A5})$$

Since an analytic expression for the final-state wave function is known in the velocity gauge, we make the standard gauge transformation [42–44]:

$$\psi_f^L = \hat{T} \psi_f^V, \quad (\text{A6})$$

where

$$\hat{T} \equiv \exp [i \mathbf{a}(t) \cdot \mathbf{r}], \quad (\text{A7})$$

where

$$\mathbf{a}(t) \equiv \frac{E_0 \cos \omega t \hat{\mathbf{e}}}{\omega} \quad (\text{A8})$$

and

$$\mathbf{r} \equiv i \nabla_{\mathbf{p}}. \quad (\text{A9})$$

Substituting Eq. (A6) into Eq. (A5), operating with \hat{T}^\dagger on $(\frac{1}{2} p^2 - \epsilon_i) |\psi_i\rangle$ using the property that \hat{T}^\dagger acts as a momentum-displacement operator [45], and taking

into account the time dependence of the initial-state wave function,

$$\psi_i(\mathbf{p}, t) = \phi_i(\mathbf{p}) e^{-i\epsilon_i t}, \quad (\text{A10})$$

we obtain

$$S_{fi}^L = i \int_{-\infty}^{+\infty} \left\langle i \frac{\partial}{\partial t} (\psi_f^V e^{i\epsilon_i t}) \middle| \hat{T}^\dagger \middle| \phi_i \right\rangle dt, \quad (\text{A11})$$

where we have used

$$i \frac{\partial}{\partial t} \psi_f^V = \frac{1}{2} (\mathbf{p} + \mathbf{a})^2 \psi_f^V. \quad (\text{A12})$$

Now the analytic solution for Eq. (A12) in momentum space is [46]

$$\psi_f^V = \delta(\mathbf{p} - \mathbf{k}_f) \exp \left(-i \left[\left(\frac{E_0 \hat{\mathbf{e}} \cdot \mathbf{k}_f}{\omega^2} \right) \sin \omega t + v \sin 2\omega t + (\epsilon_f + s)t \right] \right), \quad (\text{A13})$$

where

$$\epsilon_f = \frac{1}{2} k_f^2, \quad (\text{A14a})$$

$$v \equiv \frac{E_0^2}{8\omega^3}, \quad (\text{A14b})$$

$$s \equiv \frac{E_0^2}{4\omega^2}. \quad (\text{A14c})$$

Expanding now the harmonic dependence of the transformation operator \hat{T}^\dagger in Eq. (A7) as

$$\begin{aligned} \exp \left[-i \frac{E_0}{\omega} \cos \omega t \hat{\mathbf{e}} \cdot \mathbf{r} \right] \\ = \sum_{n=-\infty}^{\infty} (-i)^n J_n \left(\frac{E_0}{\omega} \hat{\mathbf{e}} \cdot \nabla_{\mathbf{p}} \right) e^{-in\omega t}, \end{aligned} \quad (\text{A15})$$

where the $J_n(x)$ are ordinary Bessel functions [47], and expanding the harmonic dependence of $(\psi_f^V)^\dagger$ in Eq. (A13) as

$$\begin{aligned} \exp i \left[\left(\frac{E_0 \hat{\mathbf{e}} \cdot \mathbf{k}_f}{\omega^2} \right) \sin \omega t + v \sin 2\omega t \right] \\ = \sum_{n=-\infty}^{\infty} (-1)^n J_n \left(\frac{E_0 \hat{\mathbf{e}} \cdot \mathbf{k}_f}{\omega^2}, -v \right) e^{-in\omega t}, \end{aligned} \quad (\text{A16})$$

where the $J_n(y, z)$ are generalized Bessel functions [48], one may substitute these results in Eq. (A11) and carry out the time integration to obtain

$$S_{fi}^L = \sum_N S_{fi}^L(N) \delta(\epsilon_f + s - \epsilon_i - N\omega), \quad (\text{A17})$$

where

$$S_{fi}^L(N) = 2\pi i \omega (-1)^N \sum_{n=-\infty}^{+\infty} i^n n J_{N-n} \left(\frac{E_0 \hat{\epsilon} \cdot \mathbf{k}_f}{\omega^2}, -v \right) J_n \left(i \frac{E_0}{\omega} \hat{\epsilon} \cdot \nabla_{\mathbf{k}_f} \right) \phi_i(\mathbf{k}_f). \quad (\text{A18})$$

The N -photon detachment transition amplitude is then, of course, defined by

$$T_{fi}^L(N) = -(2\pi i)^{-1} S_{fi}^L(N). \quad (\text{A19})$$

2. Low-intensity limit

Equations (A18)–(A19) give the exact Keldysh expression for the transition amplitude for detachment of an electron by a laser field. In order to make connection with the free-electron perturbation theory results (in length form) presented in Sec. III of the present paper, we take the low-intensity limit of the Keldysh transition amplitudes in Eqs. (A18) and (A19). These limits may be derived by substituting the small-argument limiting forms for both the ordinary Bessel functions and the generalized Bessel functions [49]. The result is

$$T_{fi}^L(N) = -\omega \sum_{n=1}^N (-1)^{N-n} \frac{1}{(n-1)!} A_{N-n} \left(\frac{E_0 \hat{\epsilon} \cdot \mathbf{k}_f}{\omega^2}, -v \right) \left[\frac{E_0}{2\omega} (\hat{\epsilon} \cdot \nabla_{\mathbf{k}_f}) \right]^n \phi_i(\mathbf{k}_f), \quad (\text{A20})$$

where we have defined

$$A_{N-n} = \lim_{E_0 \rightarrow 0} J_{N-n} \left(\frac{E_0 \hat{\epsilon} \cdot \mathbf{k}_f}{\omega^2}, -v \right). \quad (\text{A21})$$

Using the small-argument expressions for the generalized Bessel functions [48, 49] to evaluate A_{N-n} , we obtain the low-intensity result for the N -photon detachment amplitude in Eq. (A20). For $N = 1, 2$, and 3 , we obtain

$$T_{fi}^L(1) \xrightarrow{E_0 \rightarrow 0} \frac{E_0}{2} (\hat{\epsilon} \cdot \nabla_{\mathbf{k}_f}) \phi_i(\mathbf{k}_f), \quad (\text{A22a})$$

$$T_{fi}^L(2) \xrightarrow{E_0 \rightarrow 0} \left(\frac{E_0}{2\omega} \right)^2 \left[(\hat{\epsilon} \cdot \mathbf{k}_f) (\hat{\epsilon} \cdot \nabla_{\mathbf{k}_f}) - \omega (\hat{\epsilon} \cdot \nabla_{\mathbf{k}_f})^2 \right] \phi_i(\mathbf{k}_f), \quad (\text{A22b})$$

$$T_{fi}^L(3) \xrightarrow{E_0 \rightarrow 0} \left(\frac{E_0}{2\omega} \right)^3 \left[\frac{1}{4} \left(1 - \frac{2(\hat{\epsilon} \cdot \mathbf{k}_f)^2}{\omega} \right) (\hat{\epsilon} \cdot \nabla_{\mathbf{k}_f}) + (\hat{\epsilon} \cdot \mathbf{k}_f) (\hat{\epsilon} \cdot \nabla_{\mathbf{k}_f})^2 - \frac{\omega}{2} (\hat{\epsilon} \cdot \nabla_{\mathbf{k}_f})^3 \right] \phi_i(\mathbf{k}_f). \quad (\text{A22c})$$

One may easily confirm that these expressions are equal to those given by the free-electron perturbation theory in Eq. (32). One must simply carry through the derivatives with respect to \mathbf{k} in Eq. (32) and then relate the energy denominators to the photon frequency ω using Eq. (29).

In conclusion, we have shown the equality of the low-intensity limit of the Keldysh transition amplitude in Eq.

(A20) to the length-form perturbation-theory results (for a free-electron final state) for the particular cases $N = 1, 2$, and 3 . Mathematical proof of this equality for arbitrary values of N requires an inductive proof. However, physically we see no reason why such an equality should not hold for arbitrary N .

* Present address: University of Tennessee Medical Group, Department of Radiation Oncology, 877 Jefferson Avenue, Memphis, TN 38103-2807.

† Permanent address: Department of Physics and Astronomy, The University of Nebraska, Lincoln, NE 68588-0111.

[1] S. A. Adelman, *J. Phys. B* **6**, 1986 (1973).

[2] H. R. Reiss, *Phys. Rev. A* **22**, 1786 (1980).

[3] M. Crance and M. Aymar, *J. Phys. B* **18**, 3529 (1985).

[4] M. G. J. Fink and P. Zoller, *J. Phys. B* **18**, L373 (1985).

[5] G. P. Arrighini, C. Guidotti, and N. Durante, *Phys. Rev.*

A **35**, 1528 (1987).

[6] R. Shakeshaft and X. Tang, *Phys. Rev. A* **36**, 3193 (1987).

[7] Th. Mercouris and C. A. Nicolaides, *J. Phys. B* **21**, L285 (1988).

[8] C. Y. Tang, P. G. Harris, A. H. Mohagheghi, H. C. Bryant, C. R. Quick, J. B. Donahue, R. A. Reeder, S. Cohen, W. W. Smith, and J. E. Stewart, *Phys. Rev. A* **39**, 6068 (1989).

[9] W. W. Smith, C. Y. Tang, C. R. Quick, H. C. Bryant, P. G. Harris, A. H. Mohagheghi, J. B. Donahue, R. A.

- Reeder, H. Sharifian, J. E. Stewart, H. Toutounchi, S. Cohen, T. C. Altman, and D. C. Risolve, *J. Opt. Soc. Am. B* **8**, 17 (1991).
- [10] (a) Th. Mercouris and C. A. Nicolaidis, *J. Phys. B* **23**, 2037 (1990); (b) *ibid.* **24**, L165 (1991); (c) *Phys. Rev. A* **45**, 2116 (1992).
- [11] X. Mu, *Phys. Rev. A* **42**, 2944 (1990); X. Mu, J. Ruscheinski, and B. Craseman, *ibid.* **42**, 2949 (1990).
- [12] F. H. M. Faisal, P. Filipowicz, and K. Rzażewski, *Phys. Rev. A* **41**, 6176 (1990).
- [13] M. Crance, *J. Phys. B* **23**, L285 (1990); **24**, L169 (1991).
- [14] M. Dörr, R. M. Potvliege, D. Proulx, and R. Shakeshaft, *Phys. Rev. A* **42**, 4138 (1990).
- [15] W. Becker, S. Long, and J. K. McIver, *Phys. Rev. A* **42**, 4416 (1990).
- [16] (a) S. Geltman, *Phys. Rev. A* **42**, 6958 (1990); (b) *ibid.* **43**, 4930 (1991).
- [17] P. Lambropoulos, *Adv. At. Mol. Phys.* **12**, 87 (1976).
- [18] B. Gao and A. F. Starace, *Phys. Rev. Lett.* **61**, 404 (1988); *Phys. Rev. A* **39**, 4550 (1989).
- [19] B. Gao, C. Pan, C. R. Liu, and A. F. Starace, *J. Opt. Soc. Am. B* **7**, 622 (1990).
- [20] J. H. Macek, *J. Phys. B* **1**, 831 (1968).
- [21] U. Fano, *Rep. Prog. Phys.* **46**, 97 (1983).
- [22] C. D. Lin, *Adv. At. Mol. Phys.* **22**, 77 (1986).
- [23] A. F. Starace, in *Fundamental Processes of Atomic Dynamics*, edited by J. S. Briggs, H. Kleinpoppen, and H. O. Lutz (Plenum, New York, 1988), pp. 235–258.
- [24] C. L. Pekeris, *Phys. Rev.* **126**, 1470 (1962).
- [25] L. V. Keldysh, *Zh. Eksp. Teor. Fiz.* **47**, 1945 (1964) [*Sov. Phys. JETP* **20**, 1307 (1965)].
- [26] N. G. Basov, A. Z. Grasyuk, I. G. Zubarev, V. A. Katulin, and O. N. Krokhin, *Zh. Eksp. Teor. Fiz.* **50**, 551 (1966) [*Sov. Phys. JETP* **23**, 366 (1966)].
- [27] C. H. Park, A. F. Starace, J. Tan, and C. D. Lin, *Phys. Rev. A* **33**, 1000 (1986).
- [28] A. Dalgarno and J. T. Lewis, *Proc. R. Soc. London. Ser. A* **233**, 70 (1955).
- [29] M. Rotenberg, R. Bivins, N. Metropolis, and J. K. Wooten, Jr., *The 3-j and 6-j Symbols* (Technology Press, M.I.T., Cambridge, MA, 1959), pp. 6–7.
- [30] H. A. Bethe and C. Longmire, *Phys. Rev.* **77**, 647 (1950).
- [31] Yu. N. Demkov and G. F. Drukarev, *Zh. Eksp. Teor. Fiz.* **47**, 918 (1964) [*Sov. Phys. JETP* **20**, 614 (1965)].
- [32] M. L. Du and J. B. Delos, *Phys. Rev. A* **38**, 5609 (1988).
- [33] T. Ohmura and H. Ohmura, *Phys. Rev.* **118**, 154 (1960).
- [34] B. Gao, Ph.D thesis, The University of Nebraska – Lincoln, 1989, Appendix D.
- [35] C. J. Joachain, *Quantum Collision Theory* (North Holland, Amsterdam, 1975), Eq. (11.296).
- [36] L. S. Rodberg and R. M. Thaler, *Introduction to the Quantum Theory of Scattering* (Academic, New York, 1967), Eq. (3.59).
- [37] *Handbook of Mathematical Functions*, edited by M. Abramowitz and I. A. Stegun (Dover, New York, 1965), Sec. 10.1.
- [38] C. Pan, B. Gao, and A. F. Starace, *Phys. Rev. A* **41**, 6271 (1990).
- [39] T. F. Jiang and A. F. Starace, *Phys. Rev. A* **38**, 2347 (1988).
- [40] Compare Eqs. (51) and (38)–(40) of this paper with Eqs. (12)–(16) of Ref. 16(b).
- [41] B. Gao and A. F. Starace, *Phys. Rev. A* **42**, 5580 (1990), Sec. III A.
- [42] S. Olariu, I. Popescu, and C. B. Collins, *Phys. Rev. D* **20**, 3095 (1979).
- [43] R. R. Schlicher, W. Becker, J. Bergou, and M. O. Scully, in *Quantum Electrodynamics and Quantum Optics*, edited by A. O. Barut (Plenum, New York, 1984), pp. 405–441.
- [44] C. Cohen-Tannoudji, J. Dupont-Roc, and G. Grynberg, *Photons and Atoms: Introduction to Quantum Electrodynamics* (Wiley, New York, 1989), Sec. IV.B.3.
- [45] L. D. Landau and E. M. Lifshitz, *Quantum Mechanics*, 2nd ed. (Pergamon, Oxford, 1965), p. 45.
- [46] Cf. Ref. [41], Eqs. (2) and (7).
- [47] Cf. Ref. [37], Eqs. (9.1.5) and (9.1.7).
- [48] H. R. Reiss, *Phys. Rev. A* **22**, 1786 (1980), Appendix B.
- [49] Cf. Ref. [41], Eqs. (37), (38), and (58)–(60). Note that the latter three equations are obtained from Ref. [48].